RSC Advances

ROYAL SOCIETY OF CHEMISTRY

www.rsc.org/advances

Fine tuning of metal-specific activity in the Mn-like group of cambialistic superoxide dismutases

Irene Russo Krauss[1,2], Antonello Merlino[1,2], Andrea Pica[1,2], Rosario Rullo[3], Alessandra Bertoni[4], Alessandra Capasso[4], Massimo Amato[5], Francesco Riccitiello[6], Emmanuele De Vendittis[4], FilomenaSica[1,2*]

[1] *Dipartimento di Scienze Chimiche, Università degli Studi di Napoli Federico II, Complesso Universitario di Monte Sant'Angelo, Via Cintia, 80126 Napoli (Italy)*

[2] *Istituto di Biostrutture e Bioimmagini, CNR, Via Mezzocannone 16, 80134 Napoli (Italy)*

[3] *Istituto per il Sistema Produzione Animale in Ambiente Mediterraneo, CNR, Via Argine 1085, 80147 Napoli (Italy)*

[4]*Dipartimento di Medicina Molecolare e Biotecnologie Mediche, Università degli Studi di Napoli Federico II, Via S. Pansini 5,80131 Napoli (Italy)*

[5]*Dipartimento di Medicina e Chirurgia, Università di Salerno, Via Ponte don Melillo, 84084 Fisciano, SA (Italy)*

[6]*Dipartimento di Neuroscienze, Scienze Riproduttive e Odontostomatologiche,Università degli Studi di Napoli Federico II, Via S. Pansini 5,80131 Napoli (Italy)*

Abstract

Among Fe/Mn superoxide dismutases (SODs) a very peculiar sub-class is that of cambialistic SODs. These proteins are active with either Fe or Mn in the active site, in contrast with the other SODs that are strictly metal-specific. Here we report the metal-dependent regulation of the activity and the crystallographic structure of the cambialistic SODs from the dental pathogen *Streptococcus mutans* (SmSOD) and the food-industry bacterium *Streptococcus thermophilus* (StSOD). The two enzymes share a high sequence identity (86.2%) and present very similar three-dimensional structures. A detailed comparison with the other cambialistic SODs, found in the Protein Data Bank, allowed the identification of two sub-groups of cambialistic enzymes, the Fe-like and the Mn-like. In particular, SmSOD and StSOD were classified as belonging to the Mn-like sub-group; this assignment was in good agreement with the activity data, showing a significantly higher catalysis in Mn-bound forms of SmSOD and StSOD with respect to their Fe-forms. However, in spite of a very similar Mn-dependent activity, SmSOD and StSOD display a consistently different Fe-dependent activity, SmSOD being three-times less efficient than StSOD in the Fe-bound form. The analysis of the X-ray structures suggests that this difference could be related to the effect of a fraction of enzyme molecules possessing an atypical hexa-coordinated iron ion in the active site of SmSOD. These new structural data provide deeper insights into the family of cambialistic SODs.

Introduction

Superoxide dismutase (SOD) is a key antioxidant enzyme, catalysing the disproportionation of two toxic superoxide anions into molecular oxygen and hydrogen peroxide[1]. A metal cation bound in the active site of all SODs plays a crucial role for functioning of this enzyme. Among the structurally divergent SOD sub-families bound to different metal cofactors[1-3], Fe- and Mn-SODs constitute a homologous group, displaying its crucial role in all living kingdoms. For instance, Fe-SODs are present in primitive eukaryotes, plastids of plants and bacteria, whereas Mn-SODs occur in all the major domains of life, such as the mitochondria of eukaryotes and the cytoplasm of many bacteria[4]. This has suggested that the primitive versions of the enzyme used Fe as metal cofactor. The progression of evolution with the concurrent reduced bioavailability of the iron and its increased toxicity induced a switch to Mn-containing enzymes in the more complex organisms[5]. Together with other enzymes such as catalases and/or peroxidases, SODs participate to the cellular defence from the toxic products known as Reactive Oxygen Species (ROS) formed during the oxygen exposure of the cell[6-8]. In particular, the catalytic mechanism of superoxide dismutation is thoroughly conserved[9] and involves the sequential reduction and oxidation of the metal centre (M), with the concomitant oxidation and reduction of the two superoxide anions, following the scheme:

$$M^{3+} + O_2^{\bullet -} \rightarrow M^{2+} + O_2$$

$$M^{2+} + O_2^{\bullet -} + 2\ H^+ \rightarrow M^{3+} + H_2O_2$$

Fe-SODs and Mn-SODs share very similar primary sequences and overlapping three-dimensional structures; furthermore, they have the same residues coordinating the metal cation in the active site[9, 10]. These enzymes are organised either as homo-dimers or as homo-tetramers (dimers of dimers)[11]. The monomer is formed by two domains: a helical N-terminal domain and an α/β C-terminal domain. The active site is placed at the interface between the two domains and is formed by residues belonging to both of them: two histidines from the N-terminal domain and one aspartic acid and another histidine from the C-terminal domain[12]. A solvent molecule (water or hydroxide

depending on the pH) completes the trigonal-bipyramidal coordination geometry around the metal centre[13].

In spite of this close similarity, the presence of a selected metal (Fe or Mn) in the active site of this SOD group is in general highly specific. Indeed, the Fe bound to Fe-SODs cannot be functionally replaced by Mn; similarly, Mn-SODs do not work upon the metal exchange[11, 12, 14]. Studies performed on the Fe-substituted Mn-SOD from *Escherichia coli* showed that the active site environment induces a redox potential tuning, appropriate only for reactions with this type of metal ion. The amino acid residues responsible for the redox tuning effects have not yet been fully elucidated. This task is quite complicated, since metal selectivity and specificity arise from several synergic contributions. However, some residues important for metal selectivity have been identified, as emerging from the role of a glutamine in the second coordination sphere of SODs[5, 11]. This residue appears to be involved in determining the reduction potential of the active site, as well as the metal ion binding affinities. In particular, it belongs to the N-terminal domain of Fe-SODs (Q69 in Fe-SOD from *E. coli*) or to the C-terminal domain of Mn-SODs (Q146 in Mn-SOD from *E. coli*). Besides the diverse positioning of this residue in the amino acid sequence, no great structural differences are observed in the two different SODs[12, 14-16]. Another residue important for the specificity of these enzymes is placed more than 10 Å away from the metal centre: it is often a threonine in Fe-SODs (T154 in Fe-SOD from *E. coli*), whereas it is replaced by a glycine in many Mn-SODs[17, 18]. Indeed, mutagenic studies showed that it is possible to change the metal preference of SODs by simply mutating this residue[17]. Other residues have been classified as relevant for the Fe- or Mn-specificity, on the basis of sequence and structural alignments between known Fe- and Mn-SODs[11, 14, 18]. It is very likely that the metal-dependent specific activity of SODs is controlled by multiple factors; therefore, further studies on this subject are necessary.

Some enzymes belonging to the Fe/Mn-SOD family represent an exception to the metal-specificity rule, since they are able to function with either Fe or Mn in their active site. These enzymes, known as cambialistic SODs[19], were found in microorganisms adapted to different growth conditions,

including microaerophiles, aerobes, obligate anaerobes and also hyperthermophiles. Modern Fe-SODs and Mn-SODs are supposed to be evolved from a common ancestor *via* the family of cambialistic SODs[5]. However, our knowledge about the determinants of the specific properties of this group of enzymes is still poor, due to the scarce number of structural data available. In fact, crystal structures for only few cambialistic SODs were determined, those from the bacteria *Propionibacterium shermanii* (PsSOD)[20], *Porphyromonas gingivalis* (PgSOD)[21], and *Clostridium difficile* (CdSOD)[22, 23] and that from hyperthermophilic archaeon *Aeropyrum pernix K1* (ApSOD)[24].

Here we present the metal uptake, the metal-dependent activity and the X-ray structures of the dimeric cambialistic SODs from two *Streptococcus* species namely the dental pathogen *Streptococcus mutans* (SmSOD)[25] and the food-industry bacterium *Streptococcus thermophilus* (StSOD)[26] These microaerophiles, especially *S. mutans*, are capable of adapting their growth mechanism from anaerobic to highly oxidant conditions and we suggest that the metal-dependent regulation of the activity of streptococcal SODs could contribute to their adaptation. Furthermore, the detailed structural comparison among the known structures of cambialistic SODs, whose results enrich the knowledge on these peculiar enzymes, add new tiles to the puzzle of Fe- and Mn-SODs.

Experimental

Metal content and activity of SOD samples

Purified recombinant forms of SmSOD and StSOD were obtained through a heterologous expression system constituted by the *E. coli* BL21(DE3) strain transformed with an appropriate expression vector, vSmSOD[25] or vStSOD[26]. These pET-derived plasmids led to the production of recombinant forms of SmSOD or StSOD fused to a His-tail, useful for their one-step purification by affinity chromatography. In particular, growth of the specific BL21(DE3) transformant was carried out at 37°C in Luria-Bertani medium containing the specific antibiotic, and then the culture was induced with isopropyl-β-thiogalactopiranoside to obtain the desired recombinant product. The Mn

and Fe level in media was not controlled under these growth conditions; therefore, the uptake of these metal ions by SmSOD and StSOD probably reflected the 20:1 Fe/Mn molar ratio in growing *E. coli* cells[27]. On the other hand, the low Mn uptake by SODs did not improve, when the growth media was supplemented with 1 mg L^{-1} $MnSO_4$, as demonstrated even for a typical MnSOD[28]. The Fe and Mn content of samples of SmSOD and StSOD was determined by graphite furnace atomic absorption spectrometry with a Shimadzu ACS-6100 auto sampler, as previously indicated[29]. The detection limits for Fe and Mn were 0.1 ppb and 0.02 ppb, respectively. The improvement of Mn uptake by the cambialistic enzymes was realised through the incubation of SmSOD or StSOD (0.5 mg ml^{-1} enzyme solutions in 20 mM Tris•HCl, pH 7.8 buffer) in the presence of a final $MnCl_2$ concentration ranging between 0.05 and 1 mM. After the incubation, the protein samples were chilled on ice and an aliquot (30 µl) was loaded on a Sephadex G-50 medium column (diameter 3 mm, length 130 mm) packed in a 2-ml glass pipette, previously equilibrated at 4°C with 20 mM Tris•HCl, pH 7.8. Column was then eluted with the same buffer and 100-µl fractions were collected to separate the enzyme from the unbound divalent cation. The amount of Fe and Mn bound to the treated samples of SmSOD and StSOD was determined in the eluted fractions, which were also analysed for protein concentration and SOD activity. In particular, protein concentration was determined by the Bradford method, using bovine serum albumin as standard [30]; SOD activity was measured at 25°C in 100 mM potassium phosphate buffer, pH 7.8 and 0.1 mM Na-EDTA by the inhibition of cytochrome *c* reduction caused by superoxide anions generated with the xanthine/xanthine oxidase method[31, 32]. One unit of SOD activity was defined as the amount of enzyme that caused 50% inhibition of cytochrome *c* reduction. In the gel-filtration chromatography, the peak of enzyme activity coincided with that of bound metal cofactor and was reproducibly eluted before that of unbound metal ion.

Crystallization and data collection

Samples of SmSOD and StSOD used for crystallization experiments presented a mixed metal content. In particular, in the case of SmSOD 56% of active sites was occupied with a Fe/Mn molar ratio of 6.7, whereas in the case of StSOD 40% of active sites was occupied with a Fe/Mn molar ratio of 7.4. Initial crystallization experiments for both *Sm*SOD and *St*SOD were performed starting from crystallization conditions of other superoxide dismutases[33-35]. No satisfactory results were obtained, so sitting-drop crystallization experiments were setup at 20 °C in 96-well plates (Greiner Bio-One, Monroe, NC, USA) using an Automated Protein Crystallization Workstation (Hamilton Robotics) and precipitant solutions of commercially available crystallization screens (Hampton Research Crystal Screen 1, Crystal Screen 2 and Index). Most promising conditions were then optimized by slightly changing the concentration of precipitant agent, the pH or by adding low concentrations of poisoning agents[36]. Well diffracting crystals of StSOD grew at 20 °C from solutions containing 1.6-2.0 M ammonium sulphate and 3-5% isopropanol, using a protein concentration of 20 mg ml^{-1}. Best crystals of SmSOD grew at 20 °C from solutions containing 28-33% PEG 8000, 0.1 M sodium cacodylate buffer at pH 6.0 and 3% acetonitrile, using a protein concentration of 20 mg ml^{-1}. In both cases, the hanging drop vapour diffusion method, at a protein-to-reservoir solution ratio of 1:1 in 1-µl drops, was used. After the addition of 25% glycerol to the harvesting solution, crystals of both SODs were flash-cooled at 100 K in supercooled N_2 gas produced by an Oxford Cryosystem and maintained at 100 K during data collection. Diffraction data from StSOD were collected by using synchrotron light (λ = 1.2651 Å) at ELETTRA, Trieste, Italy and were indexed, processed and scaled with iMosflm[37]. An effective monitoring of redox states in protein crystals during data collection was not performed. However, on the basis of the literature data[38] and the X-ray exposure time (about 2 hours) the photoreduction of the ferric centres may be estimated negligible.

Crystals belong to the orthorhombic $C222_1$ space group and diffract up to 1.60 Å resolution. Matthews' coefficient calculations suggested the presence of one dimer in the asymmetric unit. In the case of SmSOD, diffraction data were collected on a Saturn944 CCD detector at the Istituto di

Biostrutture e Bioimmagini (CNR, Naples, Italy) with CuKα X-ray radiation from a Rigaku Micromax 007 HF generator and were indexed, processed and scaled with HKL2000[39]. Crystals belong to the monoclinic space group $P2_1$ and diffract up to 2.15 Å resolution. Matthews' coefficient calculations suggested the presence of two dimers in the asymmetric unit. Detailed statistics on data collections are reported in Table S1.

Structure determination and refinement

The structures of StSOD and SmSOD were solved by molecular replacement method using the program Phaser[40] and coordinates of PhSOD monomer [33] (PDB code 3LIO) as search model. To avoid bias, ions and water molecules were removed from the model. Clear solutions were obtained for both proteins. We introduced Fe as cofactor in the starting models because of the greatest percentage of this metal in the samples of proteins used for the crystal growth. The starting models were subjected to several cycles of coordinate minimization and B-factor refinement using REFMAC5[41]. Each run was alternated with manual model building using Coot[42]. The analysis of Fourier difference maps, calculated with (Fo–Fc) and (2Fo–Fc) coefficients at various stages of refinement, allowed the positioning of ions in the active sites and of several water molecules. The crystallographic R factor and Rfree for the final StSOD model, in the resolution range 30.0-1.60 Å, were 15.6% and 17.5%, respectively, whereas for SmSOD, in the resolution range 30.0-2.15 Å, were 19.3% and 25.9%. The Fe occupancy refined to unity in all cases. At the end of refinement, the geometry of protein structures was monitored using Procheck and Rampage[43]. A full list of refinement statistics is reported in Table S2. The drawings were prepared with Pymol (http://pymol.org). The coordinates of the structures have been deposited in the Protein Data Bank (Codes 4YIO for StSOD and 4YIP for SmSOD).

Sequence Alignment

Multiple alignments were performed by using the ClustalW2 on-line tool available at http://www.ebi.ac.uk/Tools/msa/clustalw2 with the BLOSUM matrix and two open gaps settings; all the other parameters were in the default setup.

Results and discussion

Metal content and uptake in SmSOD and StSOD

The presence of a specific metal cofactor (Fe or Mn) is crucial for the activity of Fe- and Mn-SODs; however, in the case of cambialistic SODs, either Fe or Mn can be incorporated into the active site of the enzyme, both metals being compatible with the functions displayed by these SODs. A previous biochemical characterization of SmSOD[25] and StSOD[26] pointed to the cambialistic nature of both enzymes and suggested a regulation of the activity by the type of bound metal cofactor. These observations prompted a deeper insight into the ability of metal uptake by SmSOD and StSOD, as well as into the metal-dependent regulation of the specific activity of these enzymes.

When measuring the metal content of untreated purified samples of the recombinant enzymes, a similar low content of Mn was found in both SmSOD and StSOD, the Mn/enzyme subunit molar ratio being 0.030 or 0.024, respectively (Table 1). This low Mn incorporation probably reflects the low availability of this metal in the growing culture of the *E. coli* heterologous expression system. A scarce Mn incorporation was measured even in a typical Mn-SOD, such as the rat mitochondrial enzyme purified from a similar heterologous expression system[28]. In contrast, the Fe content was much higher, especially for SmSOD; for instance, the Fe-enzyme molar ratio was 0.542 for SmSOD and 0.225 for StSOD. Nevertheless, all the purified protein samples had an understoichiometric total metal (Fe + Mn) content and therefore they had still empty binding sites for accommodating additional Fe or Mn.

To improve the low Mn content in SmSOD and StSOD, enzyme samples were incubated for 30 min at 30°C in the absence or in the presence of different $MnCl_2$ concentrations. The gel-filtration

chromatography of untreated and treated enzyme samples allowed the removal of excess Mn and non-specifically bound metal. Fractions containing the peak of enzyme-bound metal cofactor were collected and the results were reported in Table 1. In both SmSOD and StSOD, an improvement of the Mn content was observed after the treatment with 50 μM $MnCl_2$; at higher [$MnCl_2$] a dose-dependent increase of this metal was observed. The data suggest that SmSOD was more capable than StSOD of uptaking the Mn cation at low [$MnCl_2$], whereas an opposite trend emerged at high [$MnCl_2$]. For instance, upon treatment with 50 μM $MnCl_2$, the Mn/enzyme molar ratio raised by 2.5-fold and 1.6-fold for SmSOD and StSOD, respectively. Vice versa, after incubation with 1 mM $MnCl_2$, the ratio improved by 5.6-fold for SmSOD and 9.8-fold for StSOD. However, we cannot exclude that the differences in the Mn uptake could depend on the initial higher Fe content of SmSOD compared to that of StSOD. Concerning the Fe content measured after treatment of SmSOD and StSOD with the various $MnCl_2$ solutions, small variations were observed, less evident in the case of StSOD with respect to SmSOD. In some cases a small reduction of the Fe content was concomitant to the enhancement of the Mn uptake, whereas in other cases the level of enzyme-bound Fe increased. However, a consistent amount of Fe always remained tightly bound to both SmSOD and StSOD, as shown in Table 1. A possible cause of this variability could be the thermal treatment used for the metal exchange experiments. Under these conditions, the metal-free enzyme could transform into an insoluble structurally unfolded protein, thus leading to an apparent improvement of the Fe content with respect to the initial value. The thermophilic nature of StSOD seems in agreement with the lower variability found in this enzyme. Furthermore, the $MnCl_2$ exposure could also lead to a transient increase of apo-SOD forms. All these observations discouraged from the usage of a protocol involving the preparation of an apo-SOD form and then its reconstitution with the desired metal ion[44]. Indeed, this procedure, especially the guanidine hydrochloride treatment for the obtainment of apo-SOD forms, was unseccessful with SmSOD and StSOD, because of the occurrence of a massive protein precipitation during the denaturing treatment[25, 26].

The effect of temperature on the Mn uptake by SmSOD and StSOD was also considered. To this aim, the temperature for the 30-min incubation of the enzyme samples, in the absence or in the presence of 50 μM $MnCl_2$, was raised to 42°C (Table 1). The temperature increase favoured the Mn binding of both enzymes. Indeed, the 2.5-fold increase of the Mn molar ratio measured at 30°C for SmSOD rose to 4.9-fold at 42°C; in case of StSOD, the effect of temperature was more evident, because the Mn molar ratio increased from 1.6-fold to 4.3-fold. This finding is in line with previous reports indicating that a mild incubation temperature favoured the metal incorporation of SODs[12, 28]. The greater responsiveness of StSOD to metal uptake reflected the thermophilic behaviour of *S. thermophilus*. Concerning the Fe content measured after the incubation at 42°C, the improved metal content determined only for SmSOD is in line with the previous explanation on the effects of temperature on the less resistant enzyme from *S. mutans*.

Altogether, these data indicate that SmSOD and StSOD can improve low Mn content and that the Mn incorporation is not prevented by the high level of Fe bound to the enzymes. Temperature is beneficial for the Mn uptake of both enzymes, StSOD being more sensible to this physical parameter because of its thermophilicity.

Metal-dependent enzymatic activity of SmSOD and StSOD

Previous reports indicated that the activity of cambialistic enzymes could be regulated by the type of bound metal cofactor[22, 23, 25, 26]. To this aim, the specific activity of SmSOD and StSOD was determined before and after treatment with $MnCl_2$ solutions (Table 1). In order to correlate values of specific activity with metal content, the following equation was considered

$$Act_{tot} = (R_{Mn} \bullet Act_{Mn}) + (R_{Fe} \bullet Act_{Fe})$$

where Act_{tot} is the specific activity experimentally determined on each protein sample; R_{Mn} and R_{Fe} are the measured molar ratios of Mn and Fe, respectively; Act_{Mn} and Act_{Fe} are the specific activities extrapolated for SOD forms containing only Mn or Fe (1 mol metal/SOD subunit), respectively[25].

The values of R_{Mn}, R_{Fe} and Act_{tot} measured on the samples of SmSOD or StSOD after incubation at 30°C with the different $MnCl_2$ solutions were used to write four formulations of the equation referred to each enzyme and a matrix was constructed to extrapolate the roots Act_{Mn} and Act_{Fe}. The average values of Act_{Mn} and Act_{Fe} obtained for SmSOD were 38383 ± 3174 and 680 ± 370 U mg^{-1}, respectively; the corresponding values for StSOD were 32756 ± 4572 and 1943 ± 803 U mg^{-1}. These data clearly indicate a great metal dependent activity of SmSOD and StSOD. In particular, the increment of the Mn molar ratio observed after the enzyme incubation with $MnCl_2$ solutions caused a significant increase of the specific activity of both enzymes. Nevertheless, no significant differences were found between the Act_{Mn} values of SmSOD and StSOD, thus suggesting that a similar top level of activity was reached by the Mn-bound form of these enzymes. In contrast, the Act_{Fe} value of SmSOD was about three-times lower than that of StSOD, thus indicating that the low stimulation by Fe was even more reduced in SmSOD, compared to StSOD. As a result, the Mn-bound form of SmSOD was 56-fold more active compared to the Fe-bound form; the corresponding activity ratio calculated for StSOD was 17-times.

A similar trend was already reported in previous issues on cambialistic SODs[22, 23, 25, 26]. In particular, not only SmSOD and StSOD, but also the cambialistic SOD from *Clostridium difficile* (CdSOD) exhibited the highest activity in the Mn-bound form, even though with differences in the metal dependent activity. In the case of *Streptococcus* species, the much greater activity of the Mn-bound forms of SmSOD and StSOD could represent an adaptive response to changes of growth environments experienced by these microaerophiles. Indeed, it has been reported that growth of *S. mutans* under strong oxygen concentration absolutely requires the presence of Mn ions[45]. The significantly higher metal dependent activity exhibited by SmSOD with respect to StSOD and CdSOD probably makes this cambialistic enzyme much more adapted to environmental growth variations.

The higher activity exhibited by the Mn-bound compared to the Fe-bound form of SmSOD and StSOD could be also linked to some variations in the E^0 of these enzymes under different metal

contents. Indeed, it has been reported that a typical E^0 predicted for optimal SOD activity should be around 0.36 V, whereas that of free Fe^{3+}/Fe^{2+} or Mn^{3+}/Mn^{2+} redox couple is significantly higher, especially for the Mn couple[46]. Clearly, the metal coordination sphere of SODs depresses the redox power of the free metal couple, mainly with Mn[47, 48]. A future focus on this topic could address the possible variation of the E^0 values of cambialistic SODs under various metal contents.

Overall crystal structures of SmSOD and StSOD

The crystal structure of the cambialistic SmSOD and StSOD was determined. A full list of data-collection and refinement statistics for both SmSOD and StSOD is reported in Supplementary material, Table S1 and S2. Both cambialistic SODs adopt the topology of Fe/Mn-SODs, with the two closely similar monomers related by a dyad axis (Figure 1). Each monomer consists of two domains: the N-terminal domain, mainly made up of two long antiparallel α-helices, α1 (Ala20-Lys44) and α3 (Arg67-Leu86) connected by the short α2 (Leu52-Ala57), and the C-terminal domain, displaying a central three-stranded antiparallel β-sheet (β1 from Gly127 to Asp134 or Asn134 in SmSOD or StSOD, respectively; β2 from Lys138 to Ala145 or Pro145 in SmSOD or StSOD, respectively; β3 from Lys156 to Asp162) surrounded by helices α4 (Ala96-Phe106), α5 (Phe109-Thr122), α6 (Tyr169-Tyr172), α7 (Arg176-Glu185), α8 (from Trp189 to Leu200 or Lys200 in SmSOD or StSOD, respectively). The structures of StSOD and SmSOD are very similar to each other: root mean square deviations obtained by superposing the whole StSOD dimer to the two dimers in the asymmetric unit of SmSOD are 0.37 and 0.52 Å.

Active site

The active site of Fe/Mn-SODs is highly conserved among different members of the family: three histidines, one aspartic acid and a water molecule coordinate the metal centre in a trigonal-bipyramidal geometry (Figure 2A). The same features are observed in the two cambialistic SODs

here presented (Table 2), whose cofactor was assumed to be Fe because of the higher content of this metal in both SmSOD and StSOD samples used for the structural determination.

However, a careful analysis of electron density maps of SmSOD and StSOD active sites highlights an interesting feature in one of the subunits of SmSOD. In this case, an electron density peak at 3.3 σ level suggests the presence of an additional water molecule in *trans* position with respect to Asp162 (Figure 2B). This solvent molecule shows a lower electron density compared to the one coordinated to the Fe ion in apical position (H_2O^V). Its occupancy was manually adjusted while performing structural refinement, to obtain a B-value comparable to that of the H_2O^V[49]. Assuming a full occupation for H_2O^V (100%), the occupation of H_2O^{VI} is 40%. The Fe-H_2O^{VI} distance is longer with respect to the other distances; H_2O^{VI} lies about 1 Å out of the equatorial plane; moreover, the angles in this plane are significantly different from the canonical 90° (Table 2). There is no indication of broken or weakened bonds to the active site metal for the other ligands or any indication of dual conformations for these ligands. The Fe coordination geometry changes from a trigonal-bipyramid to a distorted octahedron. Thus, it can be supposed that in one of the two subunits of SmSOD the iron is hexa-coordinated with the additional water molecule as sixth ligand (H_2O^{VI}). The H_2O^{VI}-Fe bond length is 0.6 Å longer than that observed for the same bond in other structures of hexa-coordinatedFe-/Mn-SODs[49] and 0.5-1.0 Å longer than the distance between N and Fe in the complex of the Fe-SOD from *Pseudoalteromomas haloplanktis* with azide [33]. The H_2O^{VI} ligand is held in place by the neighbouring residues Tyr34 (H_2O^{VI}-OH 2.59 Å) and His30 (H_2O^{VI}-ND1 3.80 Å). In other Fe-/Mn-SOD structures a water molecule, which is hydrogen bonded to H_2O^{VI} and to Tyr34 side chain, is involved in preventing the escape of the sixth ligand from the active site[24, 49]. The absence of this water molecule could explain the longer distance of H_2O^{VI} from Fe and its low occupancy. These features reflect the transient nature of the Fe-H_2O^{VI} bond.

In the case of other SODs hexa-coordinated forms have been also observed in solution by spectroscopic techniques[13, 50, 51]. In particular, it has been shown that the metal ion in EcMn(II)SOD

undergoes a change from penta- to hexa-coordinated at temperatures well below 0 °C. A similar temperature-dependent conformational variation has been hypothesized in the case of the tetrameric FeSOD from the archaebacterium *Methanobacterium thermoautotrophicum*[52]. It is interesting to note that the hexa-coordinated EcMnSOD form observed in solution[53] was supposed to be different from that of the same enzyme characterized by crystallography under cryo-cooling conditions[49]. We cannot exclude that the formation of the hexa-coordinated adduct in SmSOD was induced by the temperature variation during the cooling procedure (from room temperature to 100 K). However, the similarity between the structures of the hexa-coordinated subunit of SmSOD and of EcMnSOD under cryo-trapping conditions supports the hypothesis that the present adduct mimics a SOD reaction intermediate. Significant is also the absence of any hexa-coordinated state of StSOD despite the usage of the same freezing procedure. The structural difference between SmSOD and StSOD could be involved in the enzyme mechanism. Indeed, it can be speculated that the 3-fold reduced activity of Fe-SmSOD compared to Fe-StSOD could be related to the presence of the Fe hexa-coordinated state observed only for the *S. mutans* enzyme, where the presence of H_2O^{VI} would hamper the binding of $O_2^{\bullet -}$ to the metal center. Furthermore , the observation that only the Fe-bound forms of the enzymes display such a different activity, whereas the Mn-bound forms of SmSOD and StSOD are endowed with a very similar and top-level activity could be associated with the lacking of the sixth ligand in the presence of manganese.

Comparison with the other cambialistic superoxide dismutases

Three-dimensional structures of SmSOD and StSOD were compared with those of other cambialistic SODs and the results were correlated with the structural characteristics of the Fe- or Mn-SOD subfamilies [3, 14]. The structural overlapping of cambialistic SODs (Figure 3) immediately highlights the existence of two groups: dimeric SODs (SmSOD, StSOD, CdSOD[22, 23] and PgSOD[21]) characterized by shorter α1 and α3 helices connected by the small α2 helix, and tetrameric SODs (PsSOD[20], ApSOD[24]), which lack this small helix and have longer α1 and α3 helices.

Focusing the attention on the dimeric enzymes, it emerges that the loop connecting helices α2 and α3, typically longer in Mn-SODs than in Fe-SODs, is shorter in PgSOD[21] with respect to SmSOD (Figure 4A) and also to StSOD and CdSOD (not shown).

Moving to the active site region, in particular at the second coordination sphere, other differences emerge. In particular, residues Met23, Gln147, Asp148, Gly76 and His77, found in SmSOD and StSOD and conserved in Mn-SODs[3, 11, 14], such as those from *E. coli*[49] and *Bacillus subtilis*[54], are replaced by Val, Ala, Gly, Gln and Thr in PgSOD[21] (Figure 4B), whereas in CdSOD only His77 (SmSOD coordinates) is replaced by Ala. On the other hand, all these residues are also present in Fe-SODs, such as those from *E. coli*[55] and *Plasmodium falciparum*[56].

In order to identify the signatures of metal specificity in this class of SODs, we have compared the structure of the six cambialistic enzymes with that of typical Fe- and Mn-SODs structurally organised either as dimers or as tetramers, widening our analysis beyond the global three-dimensional structure and the second coordination sphere. To this aim, Fe-SOD and Mn-SOD from *E. coli* were chosen as representative of Fe-dimer and Mn-dimer, respectively, whereas Fe-SOD from *Mycobacterium tuberculosis* (MtSOD)[57] and Mn-SOD from *Aspergillus fumigatus* (AfSOD)[58] represented Fe-tetramer and Mn-tetramer, respectively. In particular, our attention was focused on sixteen residues (Table 3), which should be characteristic of the different sub-groups of SODs[3, 11]. Interestingly, the conserved residues specific for Fe- and Mn-dependent SODs (blue and red, respectively) are absent or randomly distributed in PgSOD, PsSOD, ApSOD and CdSOD. On the other hand, SmSOD and StSOD possess almost exclusively the typical determinants of Mn-SODs; the only difference with respect to Mn-dimers, such as Mn-EcSOD or the Mn-dependent enzyme form *B. subtilis*[54], is the replacement of an arginine with an isoleucine residue at position 64 (Fe-EcSOD numbering). In Mn-dimers, this Arg strongly interacts with Asp142, which is a manganese-specific residue directly bound to another manganese-specific residue (Gln141) that belongs to the second coordination sphere and is involved in the active site hydrogen bond network [11]. This ionic pair in turn flanks the dimer-specific Asn65-Phe118 cation-π interaction[11, 14]. Thus it is possible to

classify SmSOD and StSOD, together with CdSOD, as members of the Mn-like group of cambialistic SODs, whereas PgSOD is a member of the Fe-like group.

The analysis was extended to the determinants of the oligomeric state[3, 11]. The summary of the results reported in Table 4 confirms that these structural signatures are very well defined and conserved also in cambialistic SODs.

Comparison of dimer interfaces

Catalytic activity of superoxide dismutases is crucially dependent on their quaternary structure. Dissociation of dimers into monomers results in the loss of any enzymatic activity. Thus we also performed a careful analysis of interfaces in dimeric SODs, using the cambialistic SmSOD, StSOD and PgSOD[21] and the Fe- and Mn-SOD from *E. coli*[49, 55] as references. Most of the features of SOD interface are strictly conserved among different members of the family. Interactions between the two subunits are both polar and non-polar, because involving numerous charged or aromatic residues, respectively. Moreover, due to the binary symmetry of these dimers, interactions between the two chains are perfectly symmetric. A full list of contacts in the analysed SODs is reported in Table 5; these contacts are classified as hydrophobic, hydrogen-bonded, ionic, aromatic and cation-π. The table clearly shows that, although most of the contacts are present in all proteins, a few differences exist among them. For instance, the substitution of an apolar for an aromatic residue (Tyr25 in Fe-EcSOD and Phe26 in PgSOD) adds aromatic contacts and the presence of an alanine in these two enzymes (Ala141 in Fe-EcSOD and Ala142 in PgSOD) furnishes an additional hydrophobic interaction. However, the most significant difference was found in the side chain/side chain H bonds, because of the presence of an arginine in Fe-EcSOD and in our two cambialistic SODs (Arg167 in Fe-EcSOD, Arg 173 in both SmSOD and StSOD), which is absent in Mn-EcSOD and PgSOD. This arginine forms a salt bridge with an acidic residue (Glu21 in all three SODs), strongly stabilizing the interface (Figure 5A and B), and in Fe-EcSOD it is also involved in a cation-π interaction with Tyr25. In the other two proteins (Mn-EcSOD and PgSOD) this arginine is

replaced by a glutamine that is involved in intra-chain contacts (Figure 5C). The access of Mn to the active site in apo dimeric SODs has been suggested to take place through a funnel in the dimer interface[12, 59]. Unfortunately, similar studies on the Fe access to the active are missing, so a straightforward comparison between the two classes of SOD is hindered. The presence or the lack of the strong interactions involving this arginine could be an important factor in differentiating Fe- from Mn-SODs. A multiple sequence alignment of Fe-SODs, Mn-SODs and cambialistic SODs showed that: *i*) in dimeric Fe-SODs there is a clear prevalence of arginine (it happens in 18 out of 20 cases), *ii*) in dimeric Mn-SODs there is a slightly less clear prevalence of glutamine (21 out of 31 sequences), *iii*) in cambialistic dimeric SODs arginine or glutamine are found with almost the same frequency (among the 15 analysed sequences 9 have an arginine and 6 have a glutamine), *iv*) in most tetrameric SODs there is a lysine.

Conclusion

The functional and structural characterization of two SODs from microaerophiles belonging to the *Streptococcus* genus adds new information on a simplified scheme, stating that cambialistic SODs are capable of functioning with either Fe or Mn bound into the active site. The great number of studied Fe- and Mn-SODs and the different specificity for Fe or Mn allows their location on a continuous line where strictly Fe-SODs or Mn-SODs occupy the polar positions. As a consequence, the cambialistic enzymes are located in the middle, although with a different positioning, along this line; indeed, their location should reflect a moderate preference for one metal between Fe or Mn. However, based on the global three-dimensional structure and the detailed analysis of structural determinants for metal specificity, the group of cambialistic SODs could split in two sub-groups, the Mn-like group containing SmSOD, StSOD, ApSOD and CdSOD, and the Fe-like group, containing PgSOD and PsSOD. In particular, the cambialistic SmSOD and StSOD present almost exclusively the structural features of Mn-SODs, an issue reinforced by the functional behaviour of

these enzymes, possessing a significantly higher activity in the Mn-bound compared to the Fe-bound forms. On the other hand, the cambialistic Fe-like PgSOD is endowed with an enzyme activity which is almost equal with either Fe or Mn.[17] Under this concern, SmSOD and StSOD seem to be perfectly adapted to a fine regulation of the functional activity in response to a transient shift of the growth conditions from anaerobic to highly oxidant. For instance, the very similar and high levels of activity extrapolated for the fully Mn-bound form of SmSOD and StSOD rank these enzymes at the top level among other cambialistic SODs, thus warranting the survival of these *Streptococci* under strongly oxidant conditions. Furthermore, the low Fe-specific activity is another indicator of the different adaptation of streptococcal SODs, because of the 3-fold lower activity measured with the Fe-bound form of SmSOD compared to StSOD. The characterization of the antioxidant role of the cambialistic SmSOD and StSOD, together with the preservation of the reduced state of cytosolic proteins played by the thioredoxin system in *S. mutans* and *S.thermophilus*,[60] allows a deeper insight on the adaptation of these microaerophiles to the oxidative stress.

Author Information

Corresponding Author

*E-mail: filosica@unina.it

Notes

The authors declare no competing financial interest.

Acknowledgments

Work supported by two grants from Regione Campania (Italy): L.R. 05/2008 and " Bio Industrial Processes-BIP", financed with PO FESR 2007-2013 - “Realizzazione della Rete delle Biotecnologie in Campania”.
Alessandra Bertoni was supported by a 1-year post-doctoral fellowship from CREME

project, CUP n. B25B09000050007.

We acknowledge Giosuè Sorrentino and Maurizio Amendola (Institute of Biostructures and Bioimages, CNR, Naples, Italy) for technical assistance. The staff at the crystallographic beamline of the Elettra synchrotron facility, Trieste, Italy, is also gratefully acknowledged for technical assistance.

References

1. J. J. Perry, D. S. Shin, E. D. Getzoff and J. A. Tainer, *Biochimica et biophysica acta*, 2010, **1804**, 245-262.
2. V. C. Culotta, M. Yang and T. V. O'Halloran, *Biochimica et biophysica acta*, 2006, **1763**, 747-758.
3. Y. Sheng, I. A. Abreu, D. E. Cabelli, M. J. Maroney, A. F. Miller, M. Teixeira and J. S. Valentine, *Chemical reviews*, 2014, **114**, 3854-3918.
4. M. W. Smith and R. F. Doolittle, *Journal of molecular evolution*, 1992, **34**, 175-184.
5. A. F. Miller, *FEBS letters*, 2012, **586**, 585-595.
6. J. M. Mates, *Toxicology*, 2000, **153**, 83-104.
7. J. M. McCord and I. Fridovich, *Free radical biology & medicine*, 1988, **5**, 363-369.
8. I. Fridovich, *Annual review of biochemistry*, 1995, **64**, 97-112.
9. I. A. Abreu and D. E. Cabelli, *Biochimica et biophysica acta*, 2010, **1804**, 263-274.
10. W. C. Stallings, K. A. Pattridge, R. K. Strong and M. L. Ludwig, *The Journal of biological chemistry*, 1984, **259**, 10695-10699.
11. R. Wintjens, D. Gilis and M. Rooman, *Proteins*, 2008, **70**, 1564-1577.
12. J. W. Whittaker, *Biochemical Society transactions*, 2003, **31**, 1318-1321.
13. T. A. Jackson, J. Xie, E. Yikilmaz, A. F. Miller and T. C. Brunold, *Journal of the American Chemical Society*, 2002, **124**, 10833-10845.
14. R. Wintjens, C. Noel, A. C. May, D. Gerbod, F. Dufernez, M. Capron, E. Viscogliosi and M. Rooman, *The Journal of biological chemistry*, 2004, **279**, 9248-9254.
15. J. W. Whittaker, *Methods in enzymology*, 2002, **349**, 80-90.
16. M. W. Parker and C. C. Blake, *FEBS letters*, 1988, **229**, 377-382.
17. F. Yamakura, S. Sugio, B. Y. Hiraoka, D. Ohmori and T. Yokota, *Biochemistry*, 2003, **42**, 10790-10799.
18. J. F. Bachega, M. V. Navarro, L. Bleicher, R. K. Bortoleto-Bugs, D. Dive, P. Hoffmann, E. Viscogliosi and R. C. Garratt, *Proteins*, 2009, **77**, 26-37.
19. B. Meier, D. Barra, F. Bossa, L. Calabrese and G. Rotilio, *The Journal of biological chemistry*, 1982, **257**, 13977-13980.
20. M. Schmidt, B. Meier and F. Parak, *J Biol Inorg Chem*, 1996, **1**, 532-541.
21. S. Sugio, B. Y. Hiraoka and F. Yamakura, *Eur J Biochem*, 2000, **267**, 3487-3495.
22. W. Li, H. Wang, Z. Chen, Q. Ye, Y. Tian, X. Xu, Z. Huang, P. Li and X. Tan, *Chemical communications*, 2014, **50**, 584-586.
23. W. Li, H. Wang, Q. Wang and X. Tan, *Metallomics : integrated biometal science*, 2014, **6**, 1540-1548.
24. T. Nakamura, K. Torikai, K. Uegaki, J. Morita, K. Machida, A. Suzuki and Y. Kawata, *The FEBS journal*, 2011, **278**, 598-609.
25. A. De Vendittis, M. Amato, A. Mickniewicz, G. Parlato, A. De Angelis, I. Castellano, R. Rullo, F. Riccitiello, S. Rengo, M. Masullo and E. De Vendittis, *Molecular bioSystems*, 2010, **6**, 1973-1982.

26. A. De Vendittis, S. Marco, A. Di Maro, A. Chambery, A. Albino, M. Masullo, A. Michniewicz, G. Parlato, A. De Angelis, E. De Vendittis and R. Rullo, *Protein and peptide letters*, 2012, **19**, 333-344.

27. J. E. Posey and F. C. Gherardini, *Science*, 2000, **288**, 1651-1653.

28. I. Castellano, F. Cecere, A. De Vendittis, R. Cotugno, A. Chambery, A. Di Maro, A. Michniewicz, G. Parlato, M. Masullo, E. V. Avvedimento, E. De Vendittis and M. R. Ruocco, *Biopolymers*, 2009, **91**, 1215-1226.

29. P. Montuori, P. Lama, S. Aurino, D. Naviglio and M. Triassi, *Ecotoxicology*, 2013, **22**, 295-307.

30. M. M. Bradford, *Analytical biochemistry*, 1976, **72**, 248-254.

31. A. Dello Russo, R. Rullo, G. Nitti, M. Masullo and V. Bocchini, *Biochimica et biophysica acta*, 1997, **1343**, 23-30.

32. J. M. McCord and I. Fridovich, *The Journal of biological chemistry*, 1969, **244**, 6049-6055.

33. A. Merlino, I. Russo Krauss, I. Castellano, E. De Vendittis, B. Rossi, M. Conte, A. Vergara and F. Sica, *Journal of structural biology*, 2010, **172**, 343-352.

34. A. Merlino, I. Russo Krauss, I. Castellano, E. De Vendittis, A. Vergara and F. Sica, *Protein and peptide letters*, 2008, **15**, 415-418.

35. A. Merlino, I. Russo Krauss, I. Castellano, M. R. Ruocco, A. Capasso, E. De Vendittis, B. Rossi and F. Sica, *Biochimica et biophysica acta*, 2014, **1844**, 632-640.

36. I. Russo Krauss, A. Merlino, A. Vergara and F. Sica, *International journal of molecular sciences*, 2013, **14**, 11643-11691.

37. T. G. Battye, L. Kontogiannis, O. Johnson, H. R. Powell and A. G. Leslie, *Acta crystallographica. Section D, Biological crystallography*, 2011, **67**, 271-281.

38. D. L. Tierney, J. A. Fee, M. L. Ludwig and J. E. Penner-Hahn, *Biochemistry*, 1995, **34**, 1661-1668.

39. Z. Otwinowski and W. Minor, *Method Enzymol*, 1997, **276**, 307-326.

40. A. J. McCoy, R. W. Grosse-Kunstleve, L. C. Storoni and R. J. Read, *Acta crystallographica. Section D, Biological crystallography*, 2005, **61**, 458-464.

41. G. N. Murshudov, P. Skubak, A. A. Lebedev, N. S. Pannu, R. A. Steiner, R. A. Nicholls, M. D. Winn, F. Long and A. A. Vagin, *Acta crystallographica. Section D, Biological crystallography*, 2011, **67**, 355-367.

42. P. Emsley, B. Lohkamp, W. G. Scott and K. Cowtan, *Acta crystallographica. Section D, Biological crystallography*, 2010, **66**, 486-501.

43. M. D. Winn, C. C. Ballard, K. D. Cowtan, E. J. Dodson, P. Emsley, P. R. Evans, R. M. Keegan, E. B. Krissinel, A. G. Leslie, A. McCoy, S. J. McNicholas, G. N. Murshudov, N. S. Pannu, E. A. Potterton, H. R. Powell, R. J. Read, A. Vagin and K. S. Wilson, *Acta crystallographica. Section D, Biological crystallography*, 2011, **67**, 235-242.

44. M. M. Whittaker and J. W. Whittaker, *Biochemistry*, 2008, **47**, 11625-11636.

45. M. E. Martin, R. C. Strachan, H. Aranha, S. L. Evans, M. L. Salin, B. Welch, J. E. Arceneaux and B. R. Byers, *Journal of bacteriology*, 1984, **159**, 745-749.

46. W. C. Barrette, Jr., D. T. Sawyer, J. A. Fee and K. Asada, *Biochemistry*, 1983, **22**, 624-627.

47. C. K. Vance and A. F. Miller, *Biochemistry*, 1998, **37**, 5518-5527.

48. C. K. Vance and A. F. Miller, *Biochemistry*, 2001, **40**, 13079-13087.

49. G. E. Borgstahl, M. Pokross, R. Chehab, A. Sekher and E. H. Snell, *Journal of molecular biology*, 2000, **296**, 951-959.

50. T. A. Jackson and T. C. Brunold, *Accounts of chemical research*, 2004, **37**, 461-470.

51. T. A. Jackson, A. Karapetian, A. F. Miller and T. C. Brunold, *Journal of the American Chemical Society*, 2004, **126**, 12477-12491.

52. J. P. Renault, I. Morgenstern-Badarau and M. Piccioli, *Inorganic chemistry*, 1999, **38**, 614-615.

53. L. C. Tabares, N. Cortez, I. Agalidis and S. Un, *Journal of the American Chemical Society*, 2005, **127**, 6039-6047.

54. P. Liu, H. E. Ewis, Y. J. Huang, C. D. Lu, P. C. Tai and I. T. Weber, *Acta crystallographica. Section F, Structural biology and crystallization communications*, 2007, **63**, 1003-1007.

55. M. S. Lah, M. M. Dixon, K. A. Pattridge, W. C. Stallings, J. A. Fee and M. L. Ludwig, *Biochemistry*, 1995, **34**, 1646-1660.

56. I. W. Boucher, A. M. Brzozowski, J. A. Brannigan, C. Schnick, D. J. Smith, S. A. Kyes and A. J. Wilkinson, *BMC structural biology*, 2006, **6**, 20.

57. J. B. Cooper, K. McIntyre, M. O. Badasso, S. P. Wood, Y. Zhang, T. R. Garbe and D. Young, *Journal of molecular biology*, 1995, **246**, 531-544.

58. S. Fluckiger, P. R. Mittl, L. Scapozza, H. Fijten, G. Folkers, M. G. Grutter, K. Blaser and R. Crameri, *Journal of immunology*, 2002, **168**, 1267-1272.

59. J. W. Whittaker, *Biochimica et biophysica acta*, 2010, **1804**, 298-307.

60. S. Marco, R. Rullo, A. Albino, M. Masullo, E. De Vendittis and M. Amato, *Biochimie*, 2013, **95**, 2145-2156.

Table 1 Metal content and activity of SmSOD and StSOD before and after incubation with $MnCl_2$

Enzyme	[$MnCl_2$] in the incubation mixture (µM)	Incubation temperature (°C)	R_{Mn} [a] (mol/mol)	R_{Fe} [a] (mol/mol)	Act_{tot} [b] (U/mg)
SmSOD	none	none	0.030	0.542	1475
	0	30	0.025	0.631	1404
	50	30	0.063	0.798	3204
	250	30	0.088	0.652	3552
	1000	30	0.139	0.590	5963
	0	42	0.023	0.646	1549
	50	42	0.114	0.929	8884
StSOD	none	none	0.024	0.225	1168
	0	30	0.027	0.269	1190
	50	30	0.044	0.255	2129
	250	30	0.074	0.229	2661
	1000	30	0.234	0.267	7489
	0	42	0.030	0.314	2400
	50	42	0.128	0.276	9982

[a] The Mn and Fe contents, expressed as molar ratios (R_{Mn} and R_{Fe}, respectively) with respect to the SmSOD or StSOD subunit, were determined as indicated in Material and Methods on three dilutions of each sample.
[b] The specific SOD activity (Act_{tot}) of the enzyme samples was measured in triplicates as described in Materials and Methods; proper dilutions were chosen, leading to activity values in the range 0.7 – 0.8 U mg^{-1}.

Table 2 Metal coordination geometry in the different subunits of SmSOD and StSOD.

	SmSOD (A)	SmSOD (B)	SmSOD (second dimer) (C)	SmSOD (second dimer) (D)	StSOD (A)	StSOD (B)
Bond distances (Å)						
Fe–$N^{\varepsilon 2}$ (His26)	2.15	2.23	2.07	2.16	2.09	2.16
Fe–$N^{\varepsilon 2}$ (His80)	2.20	2.29	2.28	2.27	2.09	2.11
Fe–$O^{\delta 2}$ (Asp162)	1.94	2.03	2.08	1.98	1.95	2.08
Fe–$N^{\varepsilon 2}$ (His166)	2.28	2.37	2.35	2.25	2.10	2.08
Fe–OH_2	2.15	2.25	2.28	2.01	2.37	2.29
Fe-OH_2 (2)	3.09	-	-	-	-	-
Bond angles (°)						
OH_2-Fe-$O^{\delta 2}$ (Asp162)	89.75	92.43	82.14	82.40	82.12	82.01
OH_2-Fe-$N^{\varepsilon 2}$ (His166)	91.47	88.07	82.50	90.22	91.55	92.97
OH_2-Fe-$N^{\varepsilon 2}$ (His80)	95.16	98.00	89.94	95.05	88.92	88.52
OH_2-Fe-$N^{\varepsilon 2}$ (His26)	177.98	174.39	169.63	167.96	166.57	170.04
$N^{\varepsilon 2}$ (His26)-Fe-$N^{\varepsilon 2}$ (His80)	85.31	81.12	88.78	93.37	92.94	91.48
$N^{\varepsilon 2}$ (His26)-Fe-$O^{\delta 2}$ (Asp162)	88.25	82.64	88.54	87.41	84.52	88.19
$N^{\varepsilon 2}$ (His26)-Fe-$N^{\varepsilon 2}$ (His166)	89.40	96.43	105.15	89.32	95.32	93.62
$N^{\varepsilon 2}$ (His80)-Fe-$O^{\delta 2}$ (Asp162)	94.56	108.41	108.89	102.33	103.49	100.11
$N^{\varepsilon 2}$ (His166)-Fe-$O^{\delta 2}$ (Asp162)	124.55	115.18	110.35	119.91	115.19	121.23
$N^{\varepsilon 2}$ (His80)-Fe-$N^{\varepsilon 2}$ (His166)	140.38	135.68	138.48	137.75	141.01	138.45
OH_2 (2)-Fe-$O^{\delta 2}$ (Asp162)	156.68	-	-	-	-	-
OH_2(2)-Fe-$N^{\varepsilon 2}$ (His166)	71.18	-	-	-	-	-
OH_2(2)-Fe-$N^{\varepsilon 2}$ (His80)	74.09	-	-	-	-	-
OH_2(2)-Fe-$N^{\varepsilon 2}$ (His26)	110.49	-	-	-	-	-
OH_2 (2)-Fe-OH_2	71.52	-	-	-	-	-

Table 3 Analysis of structural determinants of metal specificity in six cambialistic SODs

Residue number (1ISA numbering)	Metal specificity [a] (amino acid residue)	EcSOD (1ISA) *Fe-dependent dimer*	EcSOD (1D5N) *Mn-dependent dimer*	MtSOD (1IDS) *Fe-dependent* ***tetramer***	AfSOD (1KKC) *Mn-dependent* ***tetramer***	StSOD (4YIO) *cambialistic dimer*	SmSOD (4YIP) *cambialistic dimer*	PgSOD (1QNN) *cambialistic dimer*	CdSOD (3TJT) *cambialistic dimer*	PsSOD (1AR4) *cambialistic* ***tetramer***	ApSOD (3AK3) *cambialistic* ***tetramer***
19	MnSOD dimer (Asp)	Ser	Asp	Ser	Ser	Asp	Asp	Ser	Asp	Asp	Ile
23	MnSOD (Met)	Ile	Met	Asn	Met	Met	Met	Val	Met	Met	Met
41	MnSOD (Ala)	Leu	Ala	Ala	Ala	Ala	Ala	Leu	Ala	Ala	Ala
64	MnSOD dimer (Arg) FeSOD dimer (Phe)	Phe	Arg	Ala	Lys	Ile	Ile	Phe	Arg	Ala	Ser
67	FeSOD (Ala) MnSOD dimer (Gly)	Ala	Ala	Leu	Gly	Gly	Gly	Ala	Ala	Leu	Tyr
68	MnSOD (Gly) FeSOD (Ala)	Ala	Gly	Ala	Gly	Gly	Gly	Gly	Gly	Ala	Ala
69	FeSOD (Gln)	Gln	Gly	Gly	Gly	Gly	Gly	Gln	Gly	Gly	Gly
71	FeSOD dimer (Trp)	Trp	Ala	Val	Ile	Leu	Leu	Leu	Tyr	Val	Ile
75	FeSOD dimer (Phe)	Phe	Leu	Ile	Leu	Leu	Leu	Leu	Phe	Val	Ile
117	MnSOD dimer (Arg)	Asn	Arg	Val	Ile	Arg	Arg	Leu	Val	Ile	Val
137	MnSOD dimer (Ser)	Ser	Ser	Gln	Thr	Ser	Ser	Lys	Thr	Gln	Gln
141	MnSOD (Gln) FeSOD dimer (Ala) **FeSODs tetramer (His)**	Ala	Gln	**His**	Gln	Gln	Gln	Ala	Gln	**His**	**His**
142	MnSOD (Asp)	Gly	Asp	Gln	Asp	Asp	Asp	Gly	Asp	Gln	Asn*
143	**MnSOD tetramer (Pro)**	Thr	Ser	†	**Pro**	Thr	Thr	Asn	Ser	†	†
154	MnSOD (Gly or Ala) FeSOD (Thr or Val)	Thr	Gly	Leu	Gly	Ala	Ala	Gly	Gly	Gln	Val
165	FeSOD (Asp)	Asp	Lys	Gln	Gln	Lys	Asn*	Thr	Lys	Gln	Gln

[a] Metal specificity of the cambialistic enzymes SmSOD, StSOD, PgSOD, PsSOD and ApSOD was evaluated according to [11], using the following prototypes for metal dependence and oligomerization state: Fe-EcSOD for dimeric FeSOD, Mn-EcSOD for dimeric MnSOD, MtSOD for tetrameric FeSOD, AfSOD for tetrameric MnSOD. Conserved residues specific for FeSODs are coloured in blue, whereas those specific for MnSODs are coloured in red. Bold characters are used for tetramers. Residue numbering referred to Fe-EcSOD.

* The very similar residue Asn was found in place of Asp.

† A very different conformation was adopted in the peptide chain, and therefore it was not possible to identify a residue corresponding to Pro143.

Table 4 Analysis of structural determinants of oligomeric state in six cambialistic SODs

Residue number (1ISA numbering)	Oligomeric state [a] (amino acid residue)	EcSOD (1ISA) *Fe-dependent dimer*	EcSOD (1D5N) *Mn-dependent dimer*	MtSOD (1IDS) *Fe-dependent tetramer*	AfSOD (1KKC) *Mn-dependent tetramer*	StSOD (4YIO) *cambialistic dimer*	SmSOD (4YIP) *cambialistic dimer*	PgSOD (1QNN) *cambialistic dimer*	CdSOD (3TJT) *cambialistic dimer*	PsSOD (1AR4) *cambialistic tetramer*	ApSOD (3AK3) *cambialistic tetramer*
22	Dimer (Thr) Tetramer (Ile)	Thr	Thr	Ile	Ile	Thr	Thr	Thr	Thr	Ile	Ile
65	Dimer (Asn) Tetramer (Phe)	Asn	Asn	Phe	Phe	Asn	Asn	Asn	Asn	Phe	Phe
144	Dimer (Pro)	Pro	Pro	-	-	Pro	Pro	Pro	Pro	-	-

[a] Structural determinants of oligomeric state in the cambialistic enzymes SmSOD, StSOD, PgSOD, PsSOD and ApSOD was evaluated according to [11], using the same prototypes indicated in Table 4. Conserved residues specific for dimers are coloured in blue, whereas those specific for tetramers are coloured in red. Residue numbering referred to Fe-EcSOD.

Table 5 Comparison of interactions at the dimer interface of SmSOD, StSOD, the two dimeric SODs from *E. coli*, and the dimeric cambialistic PgSOD

	StSOD (4YIO)	**SmSOD (4YIP)**	**Fe-EcSOD (1ISA)**	**Mn-EcSOD (1D5N)**	**PgSOD (1QNN)**
Hydrophobic interactions	Leu25/Tyr169	Leu25/Tyr169	Tyr25/Tyr163	Ile25/Tyr174	Phe26/Tyr164
	Tyr34/Phe124	Tyr34/Phe124	Tyr34/Phe118	Tyr34/Phe124	Tyr35/Phe119
	-	-	Phe118/Ala141	-	Phe119/Ala142
	Phe124/Trp164	Phe124/Trp164	Phe118/Trp158	Phe124/Trp169	Phe119/Trp159
	Tyr169/Tyr169	Tyr169/Tyr169	Tyr163/Tyr163	Tyr174/Tyr174	Tyr164/Tyr164
	Tyr169/Leu170	Tyr169/Leu170	Tyr163/Ile164	Tyr174/Leu175	Tyr164/Leu165
	Leu170/Leu170	Leu170/Leu170	-	Leu175/Leu175	Leu165/Leu165
Main chain/Side chain H bonds	Ser126 (N)/ Ser126 (OG)	Ser126 (N)/ Ser126 (OG)	Ser120 (N)/ Ser120 (OG)	Ser126 (N)/ Ser126 (OG)	Ser121 (N)/ Ser121 (OG)
	Glu165 (N)/ Glu165 (OE1)	Glu165 (N)/ Glu165 (OE1)	Glu159 (N)/ Glu159 (OE1)	Glu170 (N)/ Glu170 (OE1)	Glu160 (N)/ Glu160 (OE1)
	His166 (N)/ Ser126 (OG)	His166 (N)/ Ser126 (OG)	His160 (N)/ Glu159 (OE1)	His171 (N)/ Glu170 (OE1)	His161 (N)/ Glu160 (OE1)
Side chain/Side chain H bonds	His 30 (NE2)/ Tyr 169 (OH)	His 30 (NE2)/ Tyr 169 (OH)	His 30 (NE2)/ Tyr 163 (OH)	His 30 (NE2)/ Tyr 174 (OH)	His 31 (NE2)/ Tyr 164 (OH)
	Ser126 (OG)/ Ser126 (OG)	Ser126 (OG)/ Ser126 (OG)	Ser120 (OG)/ Ser120 (OG)	Ser126 (OG)/ Ser126 (OG)	Ser121 (OG)/ Ser121 (OG)
	Glu165 (OE1)/ His166 (ND1)	Glu165 (OE1)/ His166 (ND1)	Glu159 (OE1)/ His160 (ND1)	Glu170 (OE1)/ His171 (ND1)	Glu160 (OE1)/ His161 (ND1)
	Glu165 (OE2) /His166 (ND1)	Glu165 (OE2)/ His166 (ND1)	Glu159 (OE2)/ His160 (ND1)	Glu170 (OE2)/ His171 (ND1)	Glu160 (OE2)/ His161 (ND1)
	Arg173 (NH1)/ Glu21 (OE2)	Arg173 (NE)/ Glu21 (OE2)	Arg167 (NE)/ Glu21 (OE2)	-	-
	Arg173 (NH2)/ Glu21 (OE1)	-	-	-	-
	Arg173 (NH2)/ Glu21 (OE2)	Arg173 (NH2)/ Glu21 (OE2)	Arg167 (NH2)/ Glu21 (OE2)	-	-
Ionic interactions	Glu21/Arg173	Glu21/Arg173	Glu21/Arg167	-	-
	His30/Glu165	His30/Glu165	His30/Glu159	His30/Glu170	His31/Glu160
	Glu165/His166	Glu165/His166	Glu159/His160	Glu170/His171	Glu160/His161
Aromatic interactions	-	-	Tyr25/Tyr163	-	Phe26/Tyr164
	Tyr34/Phe124	Tyr34/Phe124	Tyr34/Phe118	Tyr34/Phe124	Tyr35/Phe119
	Phe124/Trp164	Phe124/Trp164	Phe118/Trp158	Phe124/Trp169	Phe119/Trp159
Cation-Pi interactions	-	-	Tyr25/Arg167	-	-

Figure Legends

Figure 1. Cartoon representation of the SmSOD dimer. The active site residues (His26, His80, His166, Asp162) are also shown as sticks; the metal ion and the water molecule completing Fe-coordination are shown as an orange or red sphere, respectively.

Figure 2. Active site geometry. Fe ion is represented as an orange sphere, water molecules as red spheres, SOD residues as sticks. A) Common trigonal bipyramidal coordination. B) Distorted octahedral coordination found in subunit A of SmSOD. Fo-Fc omit map of H_2O^{VI} at 3.2 σ level is also shown. Lines connecting Fe-coordinating atoms are used to highlight the different coordination geometries.

Figure 3. Comparison of the monomer in different cambialistic SODs. SmSOD is cyan, StSOD yellow, PgSOD purple, CdSOD orange, PsSOD blue and ApSOD red. The metal ion in the active site is shown as an orange sphere.

Figure 4. Comparison between SmSOD (cyan) and PgSOD (purple). A) Overall 3D-structure. B) Zoom in the active site. Residues are marked according to SmSOD sequence. Where a different aminoacid is present in PgSOD it is indicated in bracket.

Figure 5. Comparison of dimer interfaces in different SODs: A) SmSOD; B) Fe-EcSOD; C) Mn-EcSOD. Glu21-Arg173 in SmSOD, and corresponding Glu21-Arg167 and Gln21-Gln178 in Fe-EcSOD and Mn-EcSOD, respectively, are shown as sticks. Residues belonging to the second subunit of the dimer are indicated with a prime symbol. Interactions between residues are explicitly shown as dash lines. Distances are in Å.

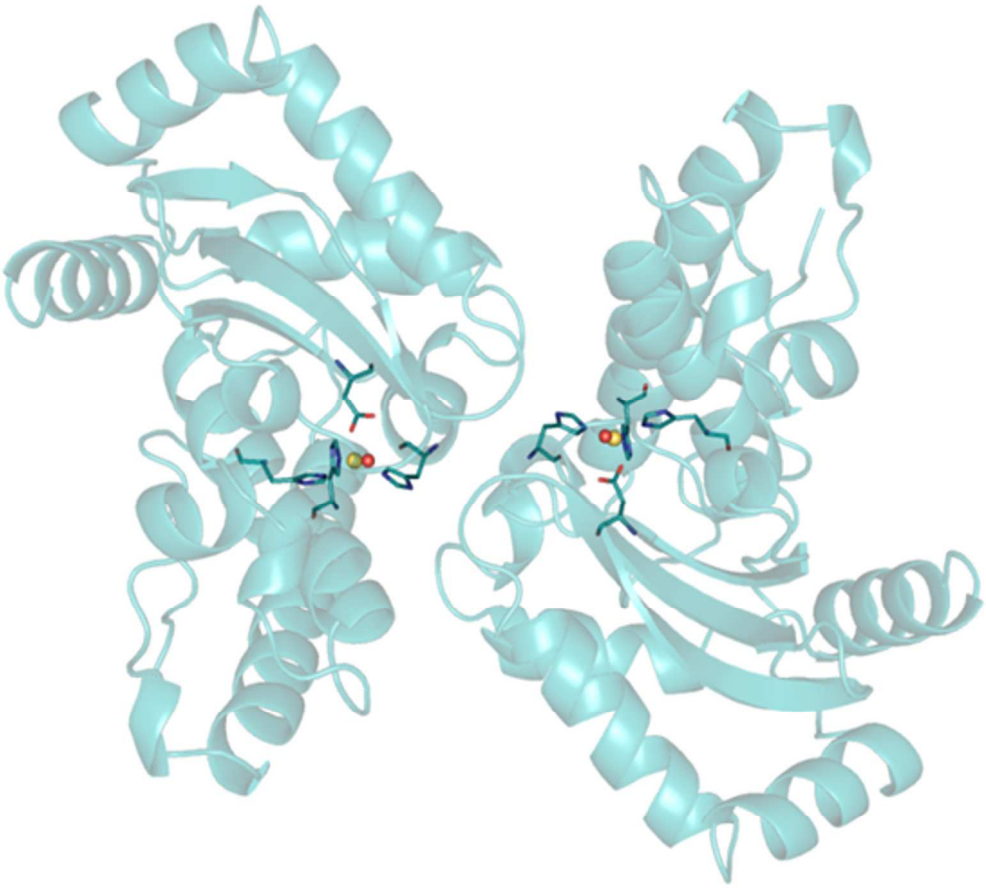

119x112mm (300 x 300 DPI)

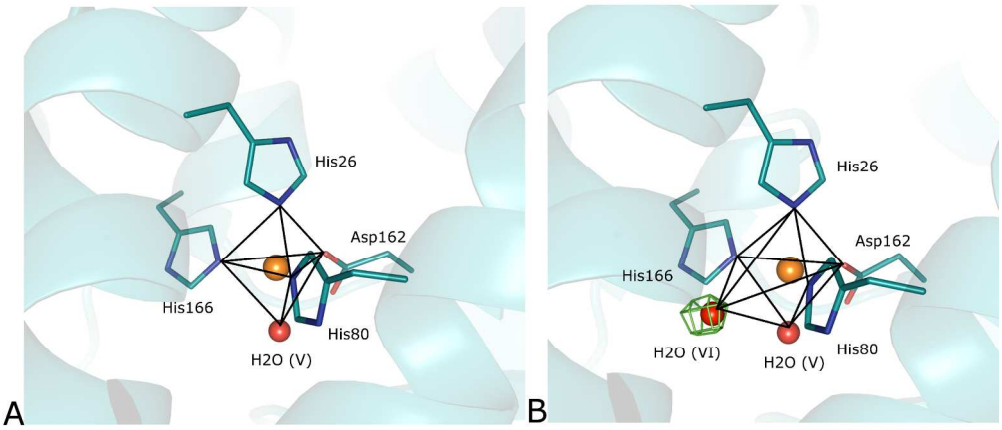

199x90mm (300 x 300 DPI)

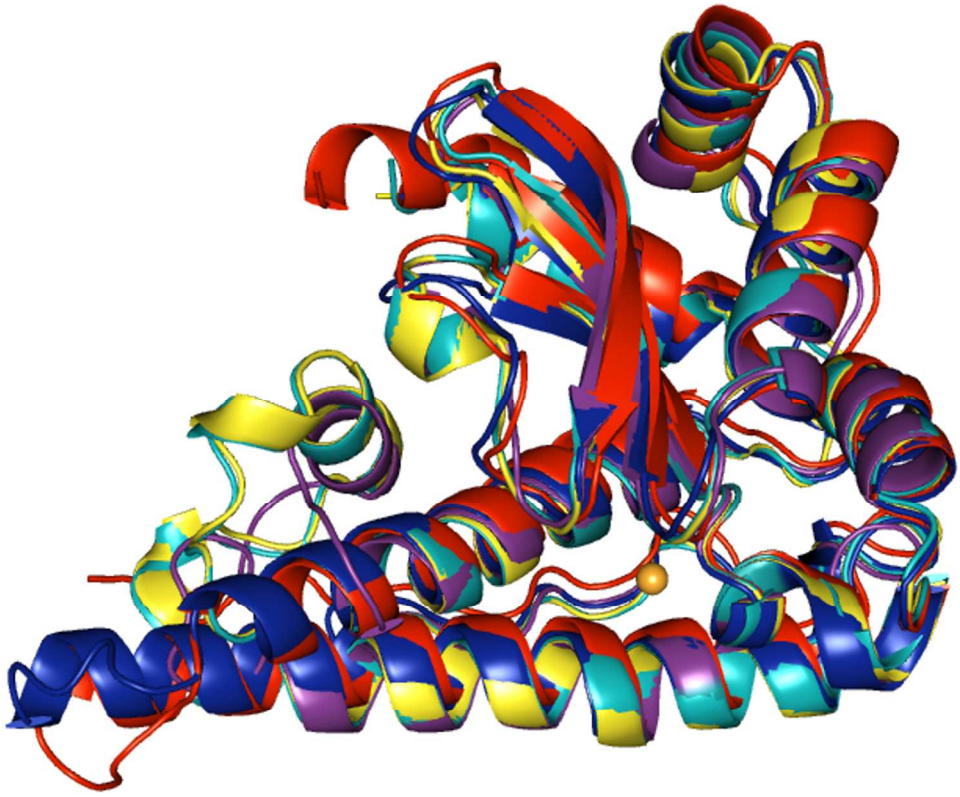

182x151mm (300 x 300 DPI)

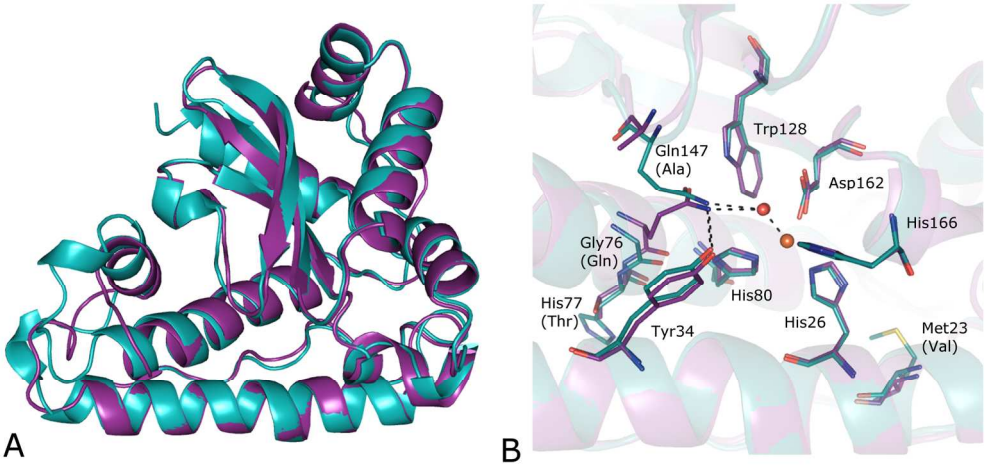

199x94mm (300 x 300 DPI)

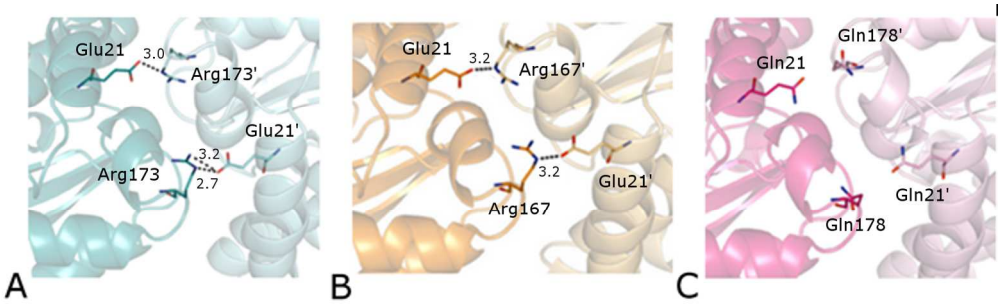

149x46mm (300 x 300 DPI)